Electronic Supplementary Material (ESI) for Journal of Materials Chemistry C.

Supporting Information

Achieve two things at one stroke: crystal engineering simultaneously optimizes emission and mechanical compliance of organic crystals

Baolei Tang, Mengjuan Li, Xu Yu, and Hongyu Zhang*

State Key Laboratory of Supramolecular Structure and Materials, College of Chemistry,

Jilin University, Changchun 130012, P. R. China. E-mail: hongyuzhang@jlu.edu.cn

General information

UV−vis absorption spectra were recorded by a Shimadzu UV-2550 spectrophotometer. The emission spectra were recorded by a Shimadzu RF-5301 PC spectrometer or a Maya2000 Pro CCD spectrometer. The absolute fluorescence quantum yields were measured on an Edinburgh FLS920 spectrometer combined with a calibrated integrating sphere. Three-point bending tests were carried out using an Instron 5944 universal testing system with a capacity of 10 N Instron 2530 load cell. Powder X-ray diffraction data were collected on a Rigaku SmartLab 3 diffractometer with Cu•Kα radiation. Scanning electron microscopy (SEM) images were obtained on the FEI Quanta 450 operated at 3 kV. All the measurements were carried out at room temperature under ambient conditions. Differential scanning calorimetric (DSC) measurements were performed on a NETZSCH DSC204 instrument at a heating rate of 10 °C min^{-1} under nitrogen. B3LYP/def-TZVP was used to do the DFT calculation via ORCA with Grimme's D3 dispersion correction. The Nanoindentation measurements were conducted using an Agilent Nano Indenter G200 with the CSM method and an XP-style actuator.

For the active optical waveguides, the crystal was irradiated by the third harmonic (355 nm) of a Nd:YAG (yttrium-aluminum-garnet) laser at a repetition rate of 10 Hz and a pulse duration of about 10 ns. The energy of laser was adjusted by using the calibrated neutral density filters. The beam was focused into a small dot by using a concentrated piece. The emission was detected at one end of the crystal using a Maya2000 Pro CCD spectrometer.

For the laser test, the crystal were irradiated by the third harmonic (355 nm) of a Nd:YAG laser at a repetition rate of 10 Hz and pulse duration of about 10 ns. The energy of the pumping laser was adjusted by using the calibrated neutral density filters. The beam was focused into a stripe whose shape was adjusted to 3.3 × 0.6 mm^2 by using a cylindrical lens and a slit. The edge emission and PL spectra of the crystals was detected using a Maya2000 Pro CCD spectrometer.

Single-crystal X-ray diffraction. Single crystal X-ray diffraction data were collected on a Rigaku RAXIS-PRID diffractometer using the ω-scan mode with graphitemonochromator Mo Kα radiation. The structures were solved with direct methods using the Olex2 programs and refined with full-matrix least squares on F^2. Non-hydrogen atoms were refined anisotropically. The

positions of hydrogen atoms were calculated and refined isotropically. The crystallographic data has been deposited with Cambridge Crystallographic Data Centre (CCDC), and signed to CCDC code 2118365 for **Cry-B**, 2118366 for **Cry-G**.

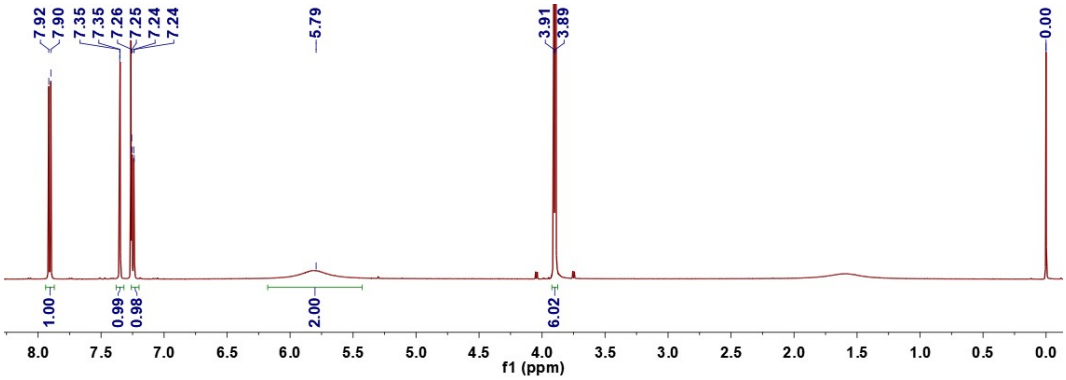

Fig. S1. ^{1}H NMR spectrum of **1** (500 MHz, $CDCl_3$).

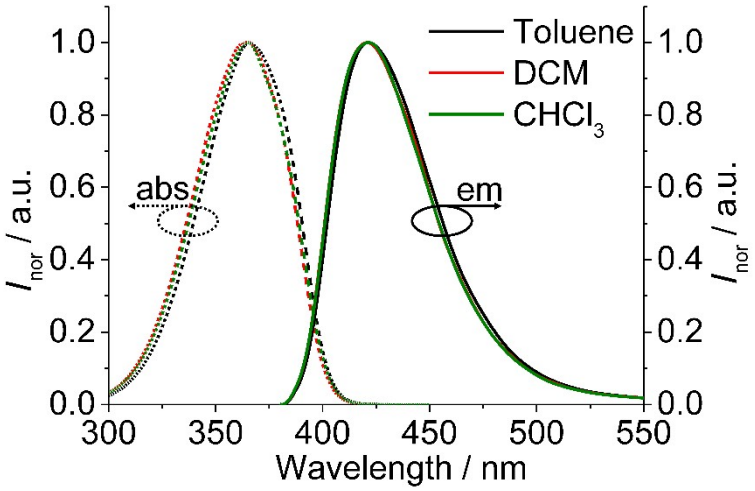

Fig. S2. Absorption (broken line) and fluorescence spectra (solid line) of **1** in solvents.

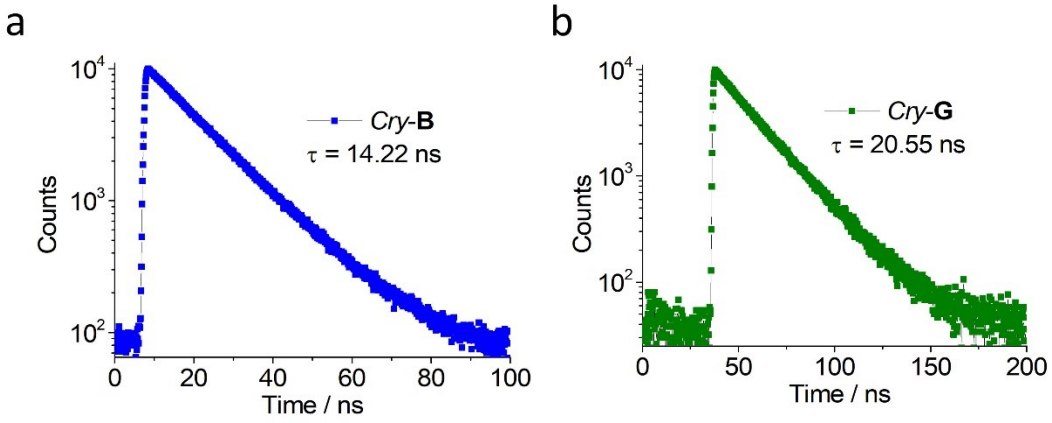

Fig. S3. Decay curves of crystals **1B** and **1G** at room temperature.

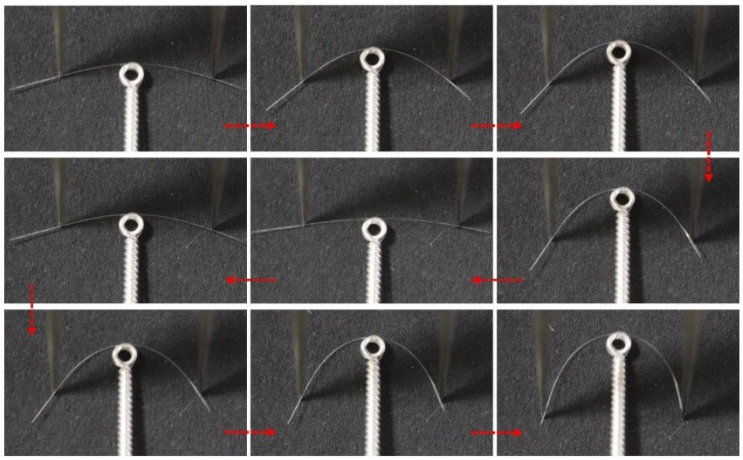

Fig. S4. Elastic bending process of crystal **1B**.

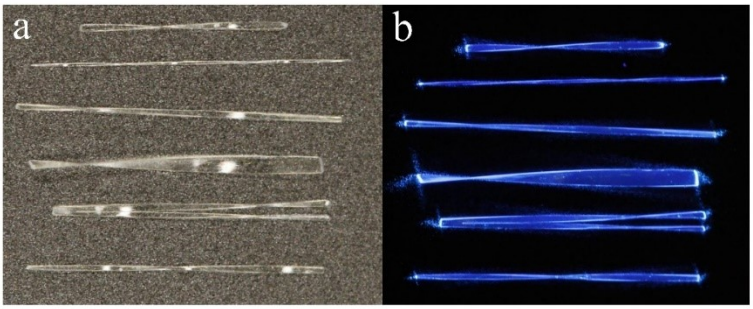

Fig. S5. Photographs of helical crystals **1B** taken under day light (a) and UV-light (b).

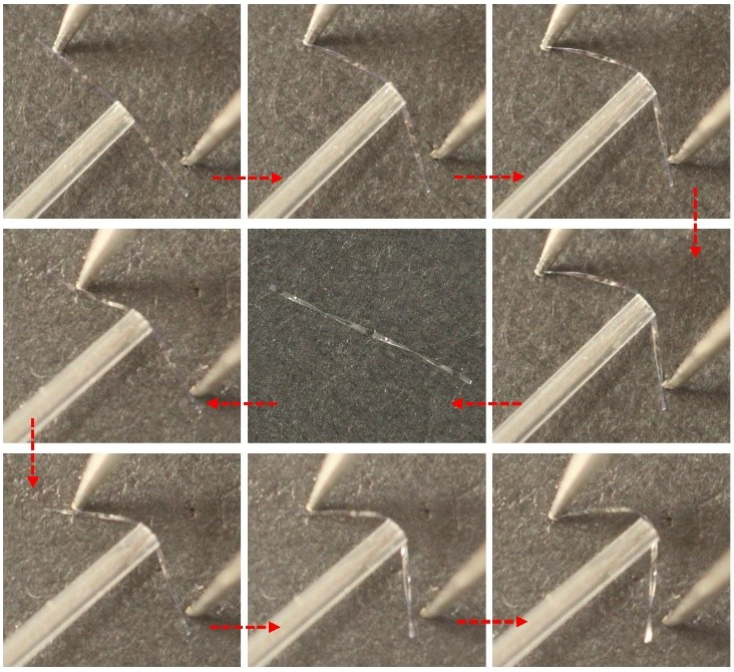

Fig. S6. Elastic bending process of helical crystal **1B**.

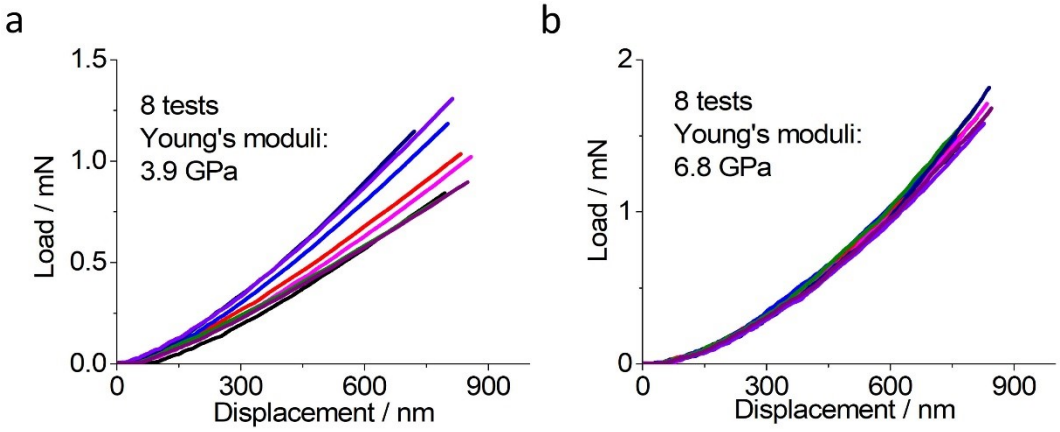

Fig. S7. Load-displacement curves obtained from the nanoindentation tests of **1B** (a) and **1G** (b).

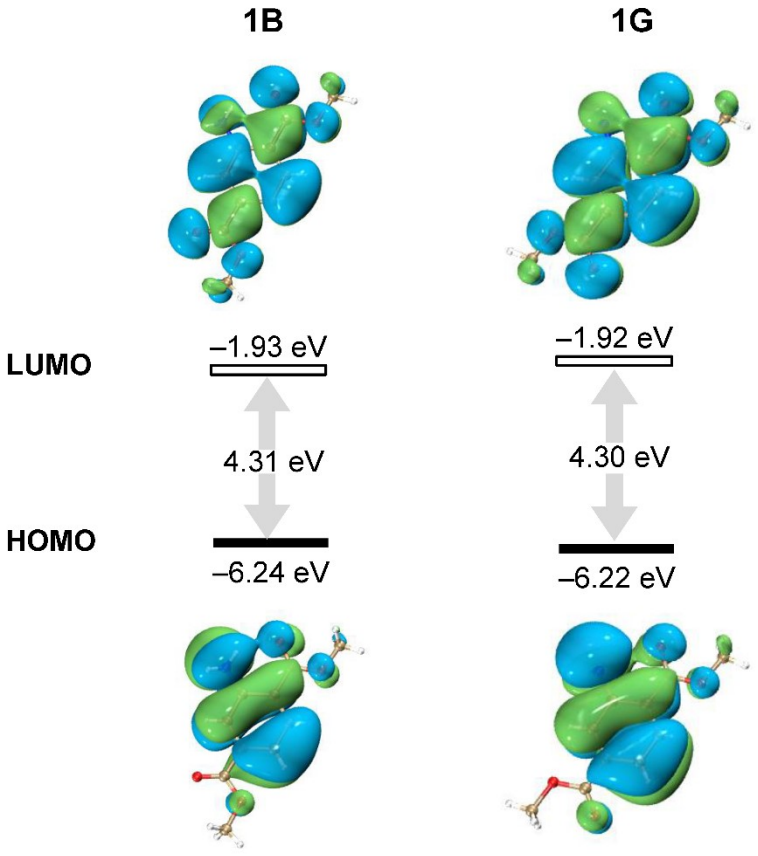

Fig. S8. The calculated energy gap between HOMO and LUMO of **1B** and **1G**.

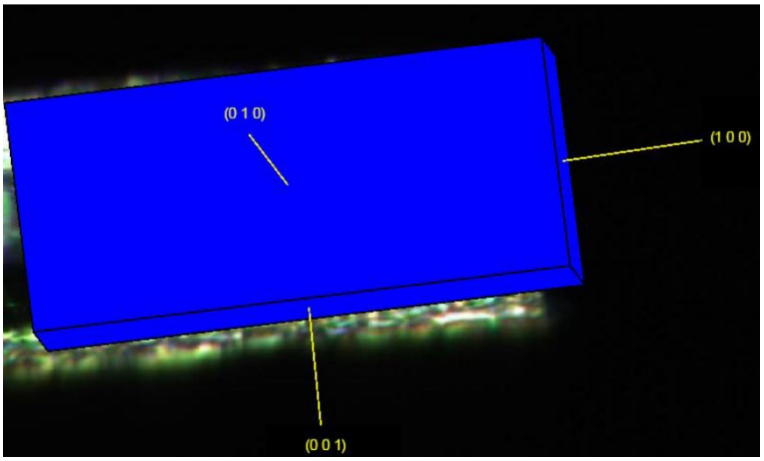

Fig. S9. Face indexing image of crystal **1B**.

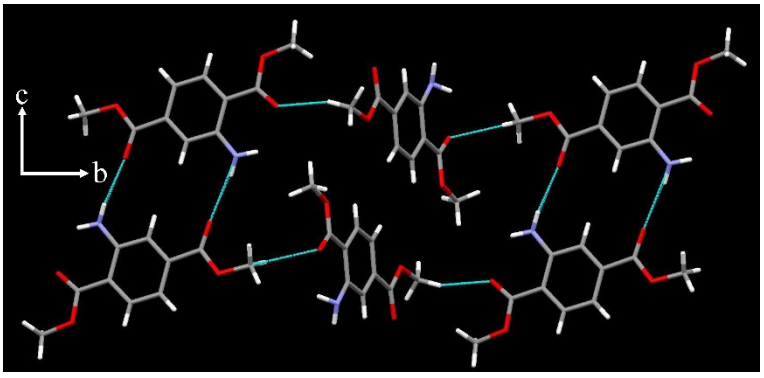

Fig. S10. Intermolecular hydrogen bonds between parallel (010) planes of crystal **1B**.

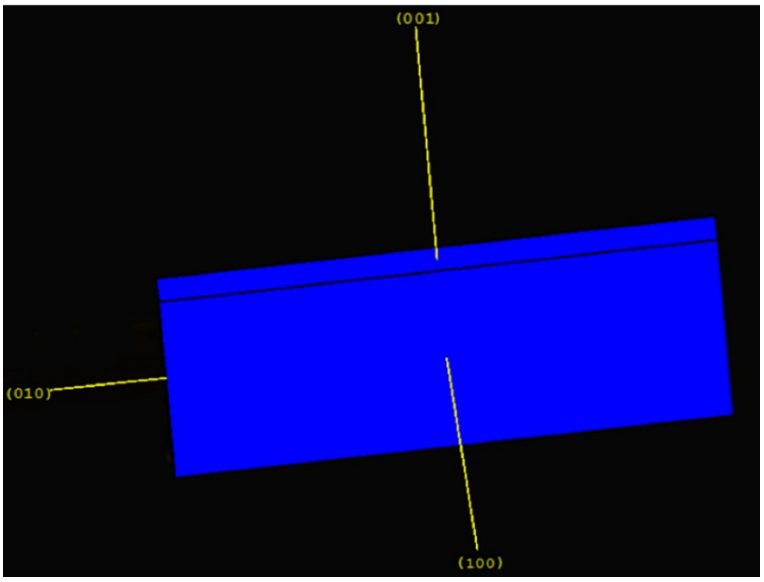

Fig. S11. Face indexing image of crystal **1G**.

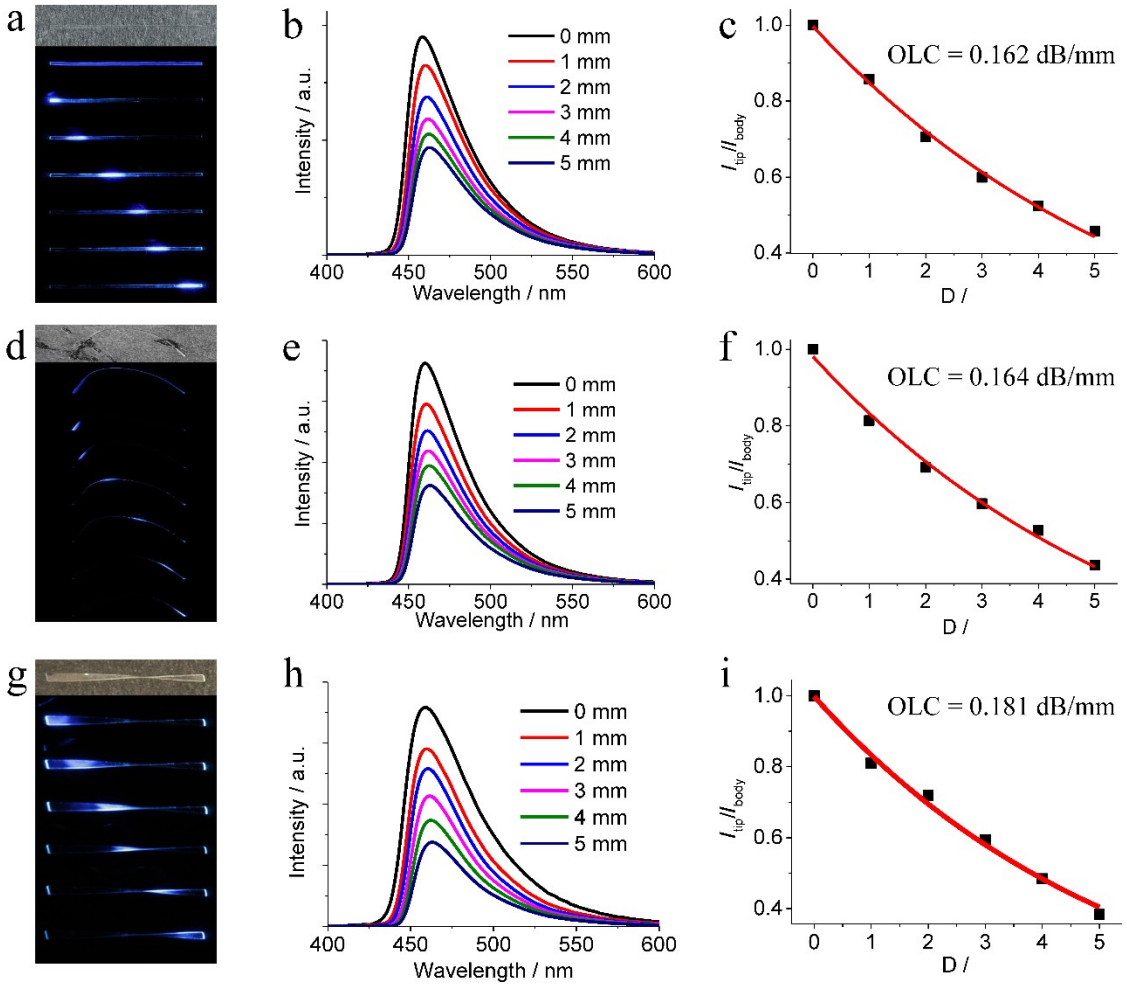

Fig. S12. Straight (a), elastically bent (d) and plastically twist (g) crystals of **1B** excited with a 355 nm laser focused at different positions. Fluorescence spectra collected at the tip of the straight (b), elastically bent (e) and plastically twist (h) crystals of **1B** with different distances between the tip and the excitation site of the laser. The I_{tip}/I_{body} decays of the **1B** straight (c), elastically bent (f) and plastically twist (i) states.

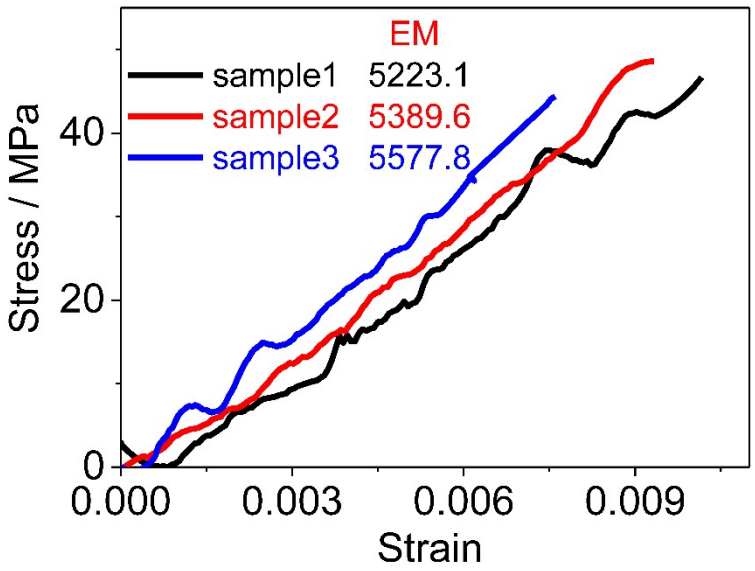

Fig. S13. Stress–strain curves obtained from three-point bending tests of three **1** crystals.

Table S1. Hydrogen bonds of crystals **1B** and **1G**

1B		**1G**	
Hydrogen bond	H•••O distance	Hydrogen bond	H•••O distance
N–H•••O(C=O)	2.201 Å	N–H•••O(C=O)	2.291 Å
C(Ph)–H•••O(C=O)	2.479 Å	$C(CH_3)$–H•••O(–O–)	2.760 Å
$C(CH_3)$–H•••O(C=O)	2.760 Å		
$C(CH_3)$–H•••O(C=O)	2.708 Å		

Table S2. Crystallographic details of crystals **1B** and **1G**.

Identification code	1B	1G
Empirical formula	$C_{10}H_{11}NO_4$	$C_{10}H_{11}NO_4$
Formula weight	209.20	210.21
Temperature/K	273.0	273.0
System	monoclinic	orthorhombic
Space group	*P*21/c	*P*ca21
a (Å)	4.7988(3)	22.016(9)
b (Å)	17.3121(13)	3.9336(15)
c (Å)	11.8745(9)	11.301(4)
α (°)	90.00	90.00
β (°)	91.415	90.00
γ (°)	90.00	90.00
V (Å^3)	986.20(12)	978.7(7)
Z	4	4
ρ_{calc} / g cm^{-3}	1.409	1.427
F (000)	440	444
Goodness-of-fit on F^2	1.045	1.070
Final R indexes	R_1= 0.0521, wR_2= 0.1272	R_1= 0.0602, wR_2= 0.1016